Detection and Analysis of Rotor Faults in Induction Motors by the Measurement of the Stray Magnetic Flux

M. Rigoni, N. Sadowski*, N. J. Batistela, J.P.A.Bastos
*GRUCAD/EEL/CTC/UFSC, P.O. Box 476, 88040-900, Florianópolis-SC, Brazil, *nelson@grucad.ufsc.br*
S. L. Nau
WEG S/A, Av. Pref. Waldemar Grubba 3300, 89256-900, Jaraguá do Sul-SC, Brazil
A. Kost
TU-Berlin, Einsteinufer 11, C-10587, Berlin, Germany

***Abstract*— This paper presents measured data and electromagnetic FEM field calculations as techniques for detecting and analyzing eccentricity in three-phase induction motors. Also it presents experimental results for detecting broken bars in induction motor rotors. A search-coil is used as magnetic field sensor to measure the stray magnetic flux outside the motor. It is a totally non-invasive method.**

***Index Terms*—**Induction motor, Eccentricity, Finite element method, Broken bars, Magnetic field sensor.

I. INTRODUCTION

Studies have shown that about 43% of electricity in Brazil is consumed by industrial plants and 56% of this energy is absorbed by electric motors [1]. Among several types of motors, the asynchronous squirrel cage one is the most employed, which is due to its low cost, robustness and maintenance easiness. Currently, with the advances on driver technologies with vector control, induction motors have increased their use on new applications.

Many evaluation studies have been performed in order to develop more accurate models and measurement systems for the failure analysis in such motors. Furthermore, within a preventive maintenance approach, it became interesting to detect potential failures before they lead to unscheduled shutdowns. Approximately 10% of failures in 100 HP (or more) induction motors occur in the cage rotor. About 40% of these cases are created by rotor bars breaking [2]. Eccentricity is also a common failure cause.

Many techniques have being proposed in the literature to detect faults in rotors [3]. Some detection ways are related to the measurements and the analysis of the temperature [4], the starting current [5], the mechanical vibration [6], the current signature analysis [2] and the instantaneous power by vector control techniques [3]. In this paper a method to detect faults in induction motors using the stray magnetic field measured outside the motor body is presented. We investigated two cases: in the first one, the motor was constructed without frame; in the second one, the machine is totally finished and possesses an iron frame involving the magnetic core.

Brazilian Microwave and Optoelectronics Society-SBMO *received 23 Aug. 2011; for review 23 Aug. 2011; accepted 9 March 2012*
Brazilian Society of Electromagnetism-SBMag *ISSN 2179-1074*

II. THE MEASUREMENT SYSTEM

The measurement system consists of a small search coil, some electronic apparatus and a computational system developed to acquire and analyze the signals of the leakage magnetic field outside the motor. The block diagram in Fig. 1 shows the whole system. They are described below.

A. The Search Coil

The used magnetic field sensor consists of a coil with a winding arranged on a plastic cylinder, with 1307 turns and an average 57.55 μm^2 cross section A_B. The external magnetic field $H(t)$ is obtained by

$$H(t) = \frac{1}{NA_B\mu_0}\int_T v(t)dt \tag{1}$$

where $v(t)$ is the induced voltage on the terminals of the sensor, N is the number of turns and μ_0 is the magnetic permeability in the air. From these structural characteristics the self inductance of the sensor is 11 mH. Fig. 2 presents the actual sensor. The sensor gain ($NA_B\mu_0$) is calibrated by a long solenoid producing an accurate known magnetic field.

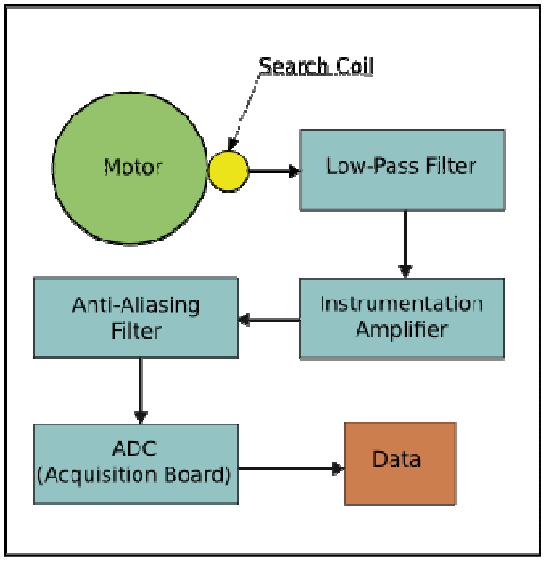

Fig.1. Block diagram of the measurement system.

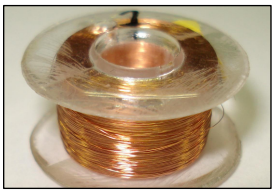

Fig. 2. The search coil.

B. Low-pass Filter

Such measurements generally present large amount of noise coupled with the sensor signal. Sometimes it has larger magnitudes compared with the signal itself. In order to acquire the information signal with good signal-to-noise ratio, an analog filter must be used prior to the

Brazilian Microwave and Optoelectronics Society-SBMO *received 23 Aug. 2011; for review 23 Aug. 2011; accepted 9 March 2012*
Brazilian Society of Electromagnetism-SBMag *ISSN 2179-1074*

amplification stage. It is a low-pass filter with bandwidth appropriated to the application. In this work an analog second-order filter was implemented using the sensor self inductance and a resistor-capacitor network whose cutoff frequency can be adjusted by changing the RC time constant value.

C. Instrumentation Amplifier

As the induced voltage amplitude on the sensor terminals is very low (ranging from some micro Volts to a few mili Volts), it is necessary to amplify the signal. Then, a Texas Instruments INA family is used. This kind of amplifier allows high values of gain (up to 60dB) with good bandwidth and high common-mode rejection [7].

D. Anti-aliasing Filter

Before the signal could be digitalized by the digital-to-analog conversion (ADC) block, an anti-aliasing filter was implemented to ensure that the signal bandwidth is restricted and satisfy the sampling theorem. The integrated circuit TLC04 from Texas Instruments, a Butterworth fourth-order low-pass filter of easy configuration, is used for this task.

E. Data Collecting

The signal sampling is obtained through a data acquisition board PCI-6251 from National Instruments. A virtual instrument was developed in the LabVIEW platform, which performs the necessary calculations to present the results by standard frequency spectrum (Fast Fourier Transform), as well as the waveforms and other relevant information. Fig. 3 shows the front panel of the developed tool.

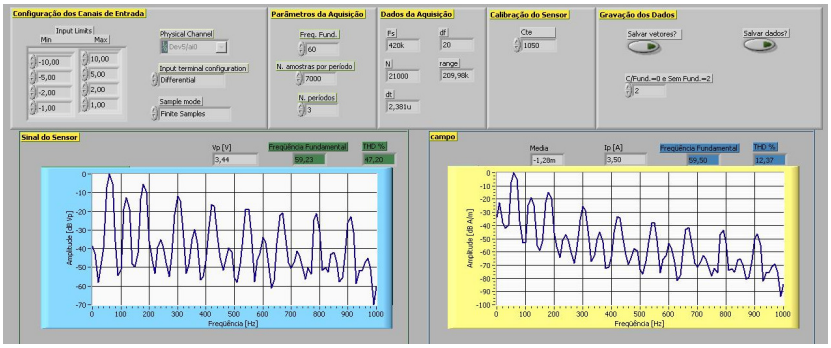

Fig. 3. Front panel of virtual instrument.

The search coil sensor is easily made and has low cost as well. As usual, it needs calibration or requires to be made by a standard process. The other electronic components have relative low costs too.

As well known, the tangential component of the magnetic field is preserved on the border of two media if there is no superficial current on it. For this reason, the leakage flux tangential component of stator penetrates the motor frame. This paper presents experimental results for a motor without frame considering eccentricity and for a complete motor with frame when broken rotor bars are present.

Brazilian Microwave and Optoelectronics Society-SBMO *received 23 Aug. 2011; for review 23 Aug. 2011; accepted 9 March 2012*
Brazilian Society of Electromagnetism-SBMag *ISSN 2179-1074*

III. EVALUATION OF STATIC ECCENTRICITY

The eccentricity, defined as the radial displacement between stator and rotor centers, plays an important role on the acoustic noise generated by three-phase induction machines [8]. It is also associated to the Unbalanced Magnetic Pull (UMP), a force that can bend the rotor towards the smaller airgap length direction. Several authors have published papers about such phenomena. For instance, in [8] the author investigates the influence of the eccentricity on the acoustic sound intensity for a 15 kW, three-phase, 4-pole induction motor with 0% and 25% eccentricity. In [9] authors state that "severe airgap eccentricity (over 25%) will contribute 2 to 3 dB(A) to the overall noise level of the machine". In [10] analytical calculations and experimental results also show the influence of the eccentricity on the acoustic noise generated by a three-phase induction motor.

In this the study, the machine presented in Fig. 4 is used. It is a three-phase induction motor having end shields and bearings specially designed to allow the radial rotor displacement and, then, to control the eccentricity. The core of the prototype is not covered by a frame in order to easily perform and measure the imposed eccentricity. This particular machine was designed by the manufacturer in order to study the eccentricity. It is a 1 hp, 8 poles, 380 V, 60 Hz motor having 36 stator slots, 44 rotor slots and 0.5 mm airgap. The large airgap was obtained by modifying the original rotor so that the eccentricities could be easily imposed (Fig. 5). In this work also Finite Element field calculations are employed instead of the analytical calculations presented in [10] in the theoretical analysis of the defects. Solely the static eccentricity is here considered.

Instead of employing common accelerometers for measuring the mechanical vibrations as in [10], external magnetic field sensors placed on the outer surface of the stator were utilized to obtain signal waveforms proportional to the derivative of the magnetic induction inside the machine.

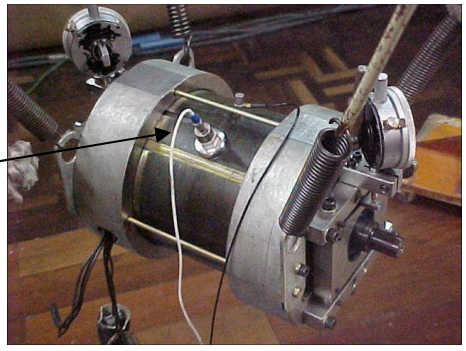

Fig.4. Motor with device to control the eccentricity on both end shields.

Brazilian Microwave and Optoelectronics Society-SBMO *received 23 Aug. 2011; for review 23 Aug. 2011; accepted 9 March 2012*
Brazilian Society of Electromagnetism-SBMag *ISSN 2179-1074*

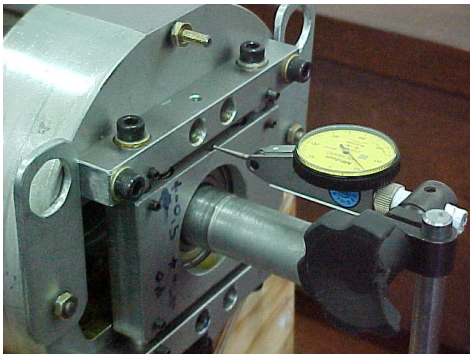

Fig. 5. Device used to impose the rotor eccentricity.

A. Finite Element Model

Two dimensional Finite Element Method coupled to electrical circuit equations are considered and, in the simulations, the induction motor is voltage fed. The Moving Band technique is used to taking into account the rotor displacement [11]. For the eccentricity study, the studied domain is the whole motor, since, for the sake of comparison, the same domain will be also used for the eccentric motor. As shown in Fig. 6, the non-eccentric rotor runs at steady state no-load operation. One can also observe, from this figure, that the magnetic flux lines are here symmetric.

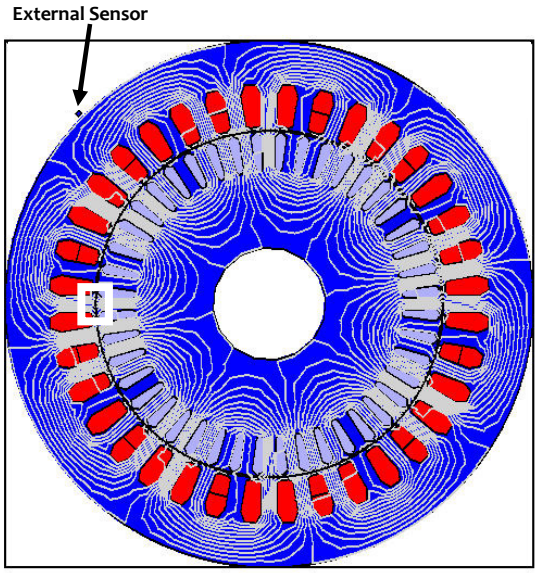

Fig. 6. Magnetic flux distribution for a non-eccentric rotor.

In this last figure the External Sensor position (for magnetic induction calculations) is indicated. From the same simulation, part of the domain is amplified and presented in Fig. 7, showing the placement of the internal airgap sensor.

Brazilian Microwave and Optoelectronics Society-SBMO *received 23 Aug. 2011; for review 23 Aug. 2011; accepted 9 March 2012*
Brazilian Society of Electromagnetism-SBMag

ISSN 2179-1074

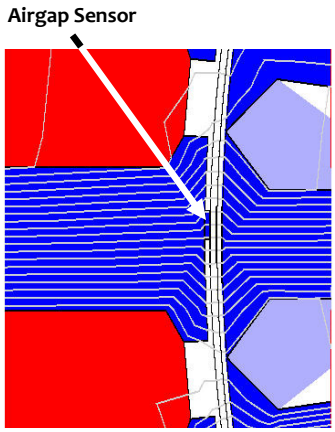

Fig. 7. Airgap sensor in FE simulations.

The non symmetric magnetic flux distribution for an eccentric rotor is now shown in Fig. 8. In this case, the rotor is displaced 0.3 mm to the right and there is, as expected, a larger flux concentration in this region as well as a lower density on the left side. Fig. 9 shows right and left airgap amplifications with their corresponding dimensions.

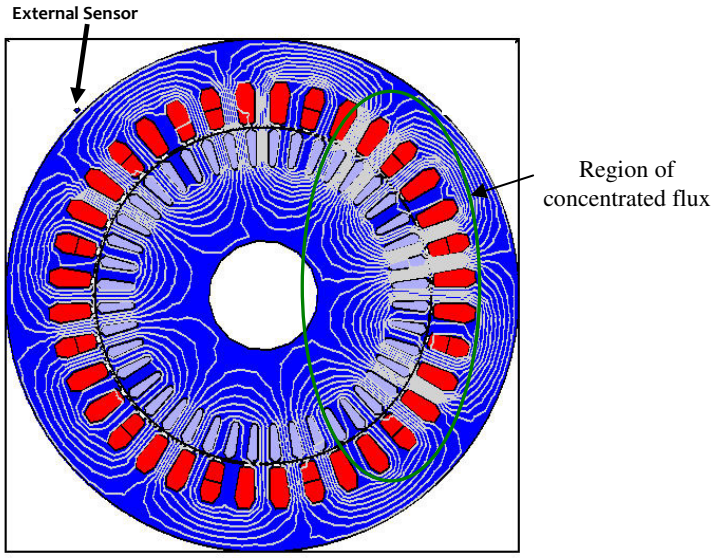

Fig. 8. Magnetic flux distribution for an eccentric rotor.

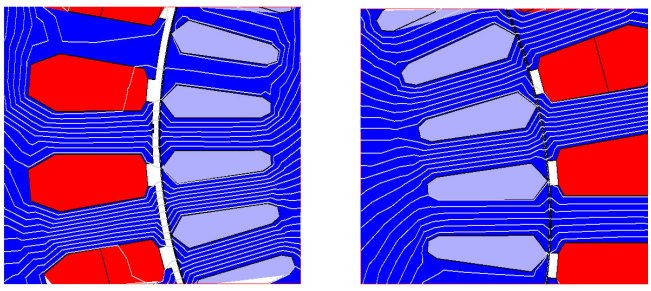

a) (b)

Fig. 9. Airgaps with a 0.3 mm eccentricity.
(al) Left airgap (0.8 mm). (b) Right airgap (0.2 mm).

B. Results

Calculation results for the radial magnetic inductions in the Airgap Sensor region at steady state no-

Brazilian Microwave and Optoelectronics Society-SBMO *received 23 Aug. 2011; for review 23 Aug. 2011; accepted 9 March 2012*
Brazilian Society of Electromagnetism-SBMag *ISSN 2179-1074*

load condition are shown in Fig. 10. As expected, there is an induction amplitude decreasing with eccentricity since the airgap in the left side is larger, compared to the right side.

Fig. 11 shows the calculated radial magnetic inductions waveforms in the External Sensor region. Here the calculation results outside the machine are used. The sensor is placed on the way that only the radial component of the magnetic induction is detected. Obviously, the magnitudes of the inductions are much lower than those shown for the airgap region in Fig. 10.

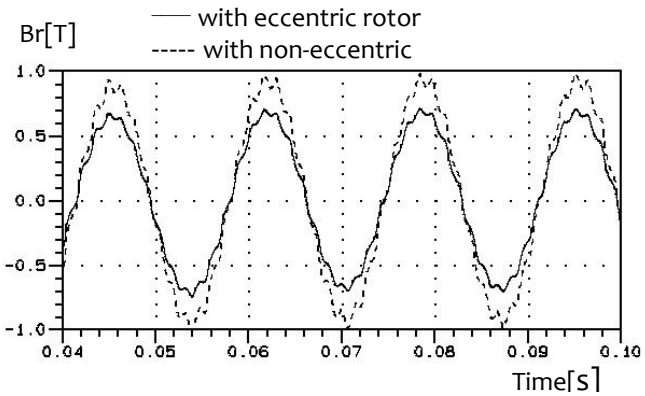

Fig. 10. Calculated radial magnetic inductions in the Airgap Sensor region at steady state conditions.

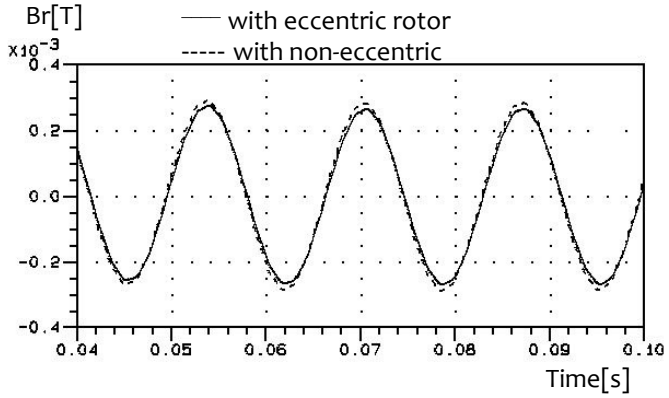

Fig. 11. Calculated radial magnetic inductions in the External Sensor region at steady state conditions.

Figures 12 and 13 present the harmonic decomposition of the curves presented in figures 10 and 11. From them, it is possible to verify that the harmonic content is nearly the same for the two sensors and, thus, the eccentricity does not generate new harmonics for the induction waveforms. On the other hand, the rotor eccentricity causes a decreasing on the amplitude of the harmonics, particularly at the 720Hz component.

Brazilian Microwave and Optoelectronics Society-SBMO *received 23 Aug. 2011; for review 23 Aug. 2011; accepted 9 March 2012*
Brazilian Society of Electromagnetism-SBMag *ISSN 2179-1074*

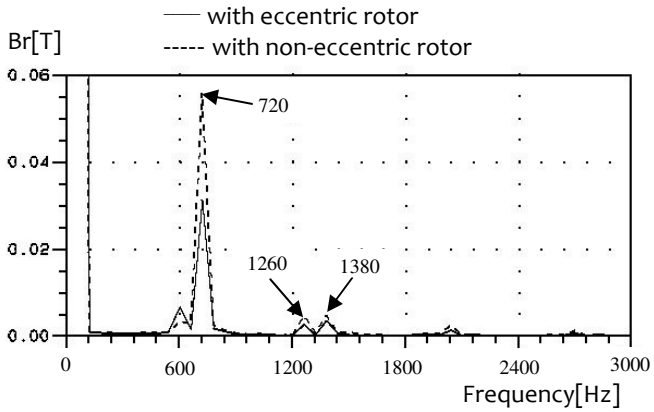

Fig. 12. Harmonics of the radial induction calculated with the Airgap Sensor.

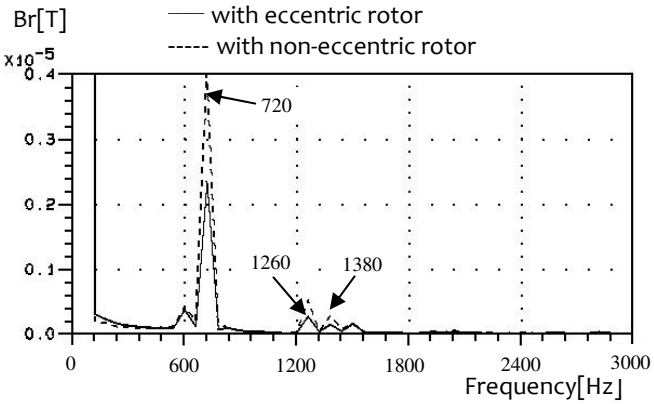

Fig. 13. Harmonics of the radial induction calculated with the External Sensor.

The harmonic content of the experimental voltage induced in the magnetic sensor is presented in Fig. 14. By comparing the results of Fig. 14 with those of figures 12 and 13 it can be noticed that 600, 720, 1260 and 1380 Hz harmonics are present on the simulation as well as on the measurements. The harmonic amplitudes are not the same because the experimental results are voltages and the calculation ones are FEM magnetic inductions. Although in quantitative aspects the amplitudes can not be directly compared, the harmonic spectra, in qualitative manner, are the same for voltages and magnetic inductions.

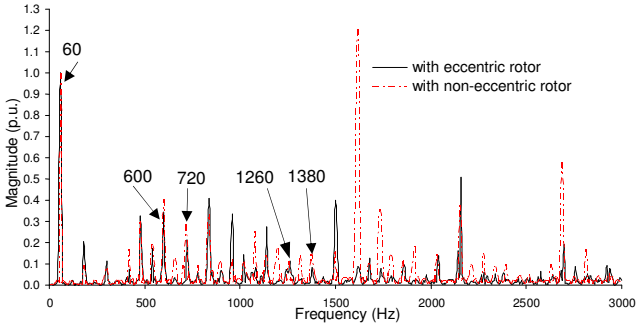

Fig. 14. Harmonics of the voltage induced in the magnetic sensor used in experimentation.

The frequencies indicated by arrows in Fig. 14 as well as in figures 12 and 13 correspond to the theoretical ones generated by rotor slots [12]:

$$f_h = f + \frac{g_2 N_2}{p}(1-s)f \tag{2}$$

where, N_2 is the number of poles, s is slip, f is the feeding frequency and $g_2 = \pm 1, \pm 2, \pm 3, \ldots$

IV. EVALUATION OF BROKEN BARS

An experimental study about the evaluation of broken bars is proposed in [13]. It is presented here to show that the above technique is able to measure the outside flux on asynchronous motor with frame as well. An electric or magnetic asymmetry in the rotor generates disturbs in the supplied electric current. Usually a frequency component located at *(1-2s)f* appears (*f* is the frequency of the excitation source and *s* is motor slip) [2], [3], [8]. Reference [3] shows that this frequency component generates a new machine torque *2sf* component, producing a change on its velocity. This variation on speed adds more distortion in the stator variables which leads to a new frequency component in the feeding electrical current, located at *(1+2s)f*.

Besides the effects on currents, asymmetries caused by the rotor bar rupture also generate disturbances in the frequency spectrum of motor leakage magnetic flux. Such distortions are also characterized by the appearance and/or the magnitude increase of certain frequencies in the spectrum. Generally, the *(1±s)f* and *(1±2s)f* frequencies magnitude are compared on normal and defective rotors. One can find papers concerning with leakage flux measurements. In [14] a round coil is placed in front of motor shielding end. With such measurements fault detections are possible but, due to the larger size of the sensor as well as to their placement, the site of the defect is more difficult to be found. Another way of measuring stray fluxes is presented in [15] where Hall effect sensors are positioned in a stator slot to investigate motor behavior with rotor broken bars.

Taking into account the constructive aspects of an electric machine, it is clear that, even in perfect condition, electric motors have some asymmetry inherent to manufacturing process. Thus, there are frequency components of *(1±2s)f* and *(1+s)f* even in motors considered "healthy", what makes difficult to identify possible failures [2], [3]. Also, the level of load and the motor size affect the magnitude of these frequency components [2].

Figure 15 shows the workbench developed in this work. The mechanical load is imposed by a Foucault braking system. It is important to emphasize that is necessary a motor firm fixation. Otherwise problems with mechanical vibration can also contribute to additional disturbances in the signal spectrum. The rotor speed is measured by an optical tachometer and also through the frequency spectrum of the voltage induced in the magnetic field sensor.

The commercial three-phase induction motor used in this broken bars investigation has the following nameplate data: 380V, 2.08A, Y connection, 60Hz, 4 poles and rated speed of 1730 rpm at 1hp. For the defective rotor tests, the same stator is kept while the normal rotor is replaced by a damaged one with three broken bars, as shown in Fig. 16. The frame of the motor is made of cast steel and the flux sensor in this study is placed on the frame as indicated in the same Fig. 16.

Brazilian Microwave and Optoelectronics Society-SBMO *received 23 Aug. 2011; for review 23 Aug. 2011; accepted 9 March 2012*
Brazilian Society of Electromagnetism-SBMag *ISSN 2179-1074*

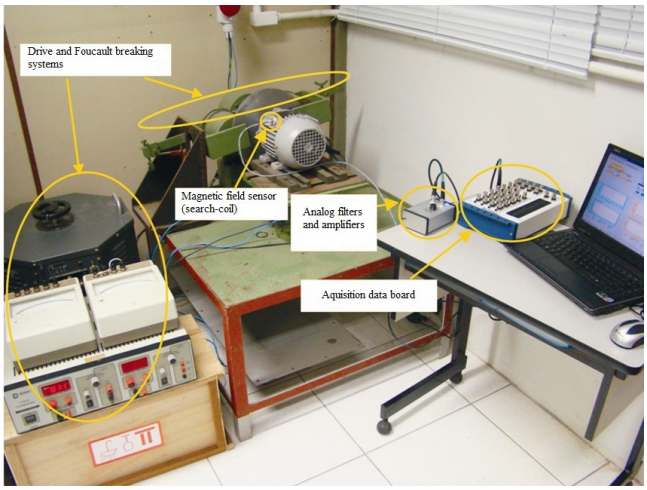

Fig. 15. Workbench employed in the studies of broken bars detection.

Fig. 16. Defective rotor.

A. Results

Regarding the broken bars detection, the different tested cases are: i) normal rotor at no-load and at full-load condition; ii) rotor with three broken bars at no-load and at full-load condition. The following figures show the measurement results through the frequency spectrum of the external magnetic field by means of FFT analysis.

The frequency spectrum of the magnetic field for the case of the normal rotor at no load is shown in Fig 17. As can be seen at the frequency range of interest, there are no different components of the fundamental frequency of 60Hz.

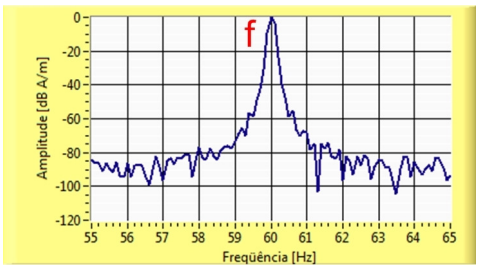

Fig. 17. Frequency spectrum of the external magnetic field for the motor using the normal rotor at no-load condition.

When mechanical load is added to the motor shaft (at full-load condition, or s=0.0333), a frequency

received 23 Aug. 2011; for review 23 Aug. 2011; accepted 9 March 2012

ISSN 2179-1074

component of *(1-s)f* appears in the stray magnetic flux spectrum (see Fig. 18). This component is due to the rotating field produced by rotor currents.

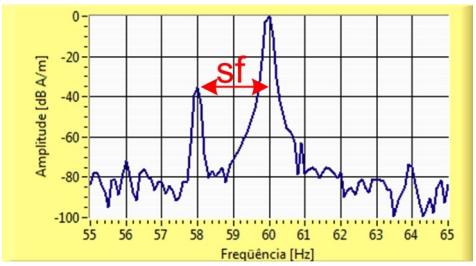

Fig. 18. Frequency spectrum of the external magnetic field for the motor using the normal rotor at full-load condition.

As stated above, the other frequency components at *(1+s)f* and *(1±2s)f* are not expected for a healthy rotor. For a *s*=0.0333 slip, these components may occur at 56Hz, 62Hz and 64Hz in the case of a broken bars rotor. From Fig. 18, one observes that the components at 56 Hz, 62 Hz and 64 Hz have, respectively, amplitudes of -72.15 dB, -38.07 dB and -73.77 dB which could be neglected for the normal rotor.

Considering now the test for the three broken bars rotor, at no-load operating, the frequency spectrum from the external magnetic field measurement is quite similar to that for the normal rotor, as in Fig. 19. Only the fundamental component at 60Hz is evident. There are no induced currents in the rotor with sufficient amplitude to generate a detectable reaction of magnetic unbalance.

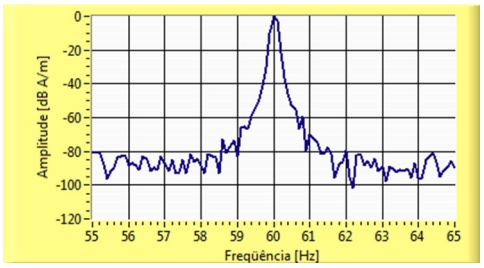

Fig. 19. Frequency spectrum of the external magnetic field for the motor using the defective rotor at no-load condition.

However, when the full-load condition is imposed there are components for the frequencies of 56.2 Hz (-44.5dB) and 63.9 Hz (-49.3 dB), shown in Fig. 20. It is clear that there are substantial increases in the magnitude of these components, compared to the same load condition for the normal rotor. In this case there is also a component of relatively low amplitude *(1+s)f* (61.9 Hz) which, nevertheless, has a lower amplitude compared to the other ones.

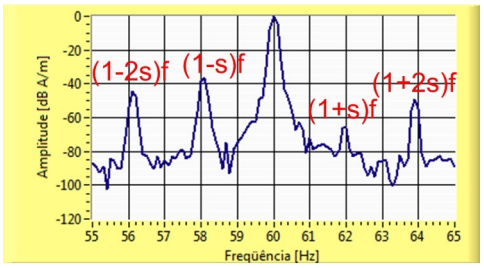

Fig. 20. Frequency spectrum of the external magnetic field for the motor using the defective rotor at full-load condition.

Brazilian Microwave and Optoelectronics Society-SBMO *received 23 Aug. 2011; for review 23 Aug. 2011; accepted 9 March 2012*
Brazilian Society of Electromagnetism-SBMag

ISSN 2179-1074

V. CONCLUSION

Two dimensional Finite Element simulations and experimental procedures are used in this work for analyzing static eccentricity in a three-phase squirrel cage induction motor. An experimental study is also carried out for rotor broken bars. Search coil sensors signals are employed to measure the magnetic field outside the machine. When carefully treated, they furnish important information concerning the motor functioning without the need of installing sensors internally in the machine, a difficult task in practical applications.

Besides the measuring data, Finite Element calculations as well as analytical equations can provide some additional information pointing out and distinguishing, in the experimental harmonic spectrum, the frequencies of electromagnetic origin from the others ones arising from external sources as well as those of mechanical origin.

One of the goals is to assess studies presented by the references [2], [3], [10] by means of the proposed measurement system. This paper shows that broken bars and static eccentricity can be detected based on magnetic field sensors placed outside of electrical machine.

The main advantage of the methodology proposed in this paper, when compared to other ones found in the literature, is that it is not intrusive. It is based on magnetic field sensors that are placed outside of the electrical machine. It is important to notice that the experimental results show that this proposed system works satisfactorily for motor with or without frame. It enables to check possible constructive troubles and it is a highly convenient procedure for industrial applications.

REFERENCES

[1] http://www.procobre.org/pr/pdf/pdf_pr/08.pdf, April, 2008.

[2] Ahmed, I.; Ertugrul, N.; Soong, W.L. A Study on the Fault Frequencies for Condition Monitoring of Induction Machines. AUPEC 2005. Australasin Universities Power Engineering Conference. Hobart, Tasmania, Australia.

[3] Bellini, A.; Filippetti, F.; Franceschini G.; Tassoni, C.; Kliman, G.B.; Quantitative Evaluation of Induction Motor Broken Bars by Means of Electrical Signature Analysis. IEEE Trans. on Ind. Appl., vol. 37, no. 5, Sep./Oct. 2001, pp. 1248-1255.

[4] Yahoui H., Jammal A., Grellet G. Thermal Monitoring of three phases cage Asynchronous Machines. ICEM 1994, France. Proceedings of International Conference on Electrical Machines. Paris 1994, vol.2, p. 278-281

[5] Supangat, R.; Ertugrul, N.; Soong, W.L.; Gray, D.A.; et al. Broken Rotor Bar Fault Detection in Induction Motors Using Starting Current Analysis. Proceedings of the 11th European Conference on Power Electronics and Applications, Dresden, 2005.

[6] Rodríguez, P. V. J. Current-, *Force-, and Vibration-Based Techniques for Induction Motor Condition Monitoring*, Dissertation for the degree of Doctor of Science in Technology. University of Technology, Espoo, 2007.

[7] Rigoni, M., Antonio Junior, A. C., Santos, T. L. dos, Batistela, N. J., Sadowski, N. A differential analog amplification circuit for small signals from induction coil sensors. In: Soft Magnetic Materials 19, Sep. 2009, Torino, p. M3-09.

[8] Maliti K. C., *Modelling and Analysis of Magnetic Noise in Squirrel-Cage Induction Motors*, Doctoral Dissertation, Royal Institute of Technology, Department of Power Engineering, Electrical Machines and Power Electronics, Stockholm, 2000.

[9] Bonnet A. H. , G. C. Soukup, Cause and analysis of stator and rotor failures in three-phase squirrel-cage induction motors, IEEE Trans. on Industry Applications, Vol. 28, N. 4, July/August 1992, pp. 921-937.

[10] Nau S. L., R. Beck, N.Sadowski, The influence of the eccentricity on the magnetic noise of three-phase induction motor: an experimental approach, Proceedings of ICEM 2004, September 05-08, Cracow, pp. 412-416..

[11] J.P.A.Bastos, N.Sadowski, *Electromagnetic Modeling by Finite Element Methods*, Marcel Dekker, New York, 2003.

[12] S. L. Nau, R. Beck, H. L. V. dos Santos, N.Sadowski, R.Carlson, The increase of the magnetic noise of induction motors due to the low order excitation models generated by the rotor eccentricity, Conference Papers of ICEM 2006, September 02-05, Crete, pp. 1-6 (CD).

[13] Rigoni, M.; Santos, T. A.; Santos, A. L., Sadowski, N., Batistela, N. J. Estudo Experimental da Detecção de Defeitos em Rotores em Gaiola por meio do Campo Externo. In: 13º SBMO Simpósio De Microondas e Optoeletrônica/8º CBMAG Congresso Brasileiro de Eletromagnetismo, Florianópolis, p. 166-170, 2008, (in Portuguese).

Brazilian Microwave and Optoelectronics Society-SBMO *received 23 Aug. 2011; for review 23 Aug. 2011; accepted 9 March 2012*
Brazilian Society of Electromagnetism-SBMag *ISSN 2179-1074*

[14] Siau, F., Graff, A., Soong, W., Ertugrul, N., Broken Bar Detection in Induction Motors Using Current and Flux Spectral Analysis. Australian Journal of Electrical & Electronics Engineering, Vol. 1, No. 3, 2004, pp. 171-177.
[15] C. G. Dias, I. E. Chabu, M. A. Bussab, Hall Effect Sensor and Artificial Neural Networks Applied on Diagnosis of Broken Rotor Bars in Large Induction Motors, Proceedings of CIMSA 2006, July 12-14, La Coruna, pp. 34-39.

Brazilian Microwave and Optoelectronics Society-SBMO *received 23 Aug. 2011; for review 23 Aug. 2011; accepted 9 March 2012*
Brazilian Society of Electromagnetism-SBMag *ISSN 2179-1074*